

# Dynamic Introduction of Cell Adhesive Factor via Reversible Multicovalent Phenylboronic Acid/*cis*-Diol Polymeric Complexes

Guoqing Pan,<sup>\*,†,‡,§</sup> Bingbing Guo,<sup>†,‡</sup> Yue Ma,<sup>||</sup> Wenguo Cui,<sup>†,‡</sup> Fan He,<sup>†,‡</sup> Bin Li,<sup>†,‡</sup> Huilin Yang,<sup>†,‡</sup> and Kenneth J. Shea<sup>§</sup>

<sup>†</sup>Orthopedic Institute, Soochow University, 708 Renmin Road, Suzhou, Jiangsu 215007, China

<sup>‡</sup>Department of Orthopaedics, The First Affiliated Hospital of Soochow University, 188 Shizi Street, Suzhou, Jiangsu 215006, China

<sup>§</sup>Department of Chemistry, University of California, Irvine, California 92697, United States

<sup>||</sup>Department of Chemistry, Nankai University, Tianjin 300071, China

## S Supporting Information

**ABSTRACT:** In this work, dynamic introduction of bioactive RGD peptide on a matrix was successfully demonstrated via reversible multicovalent interactions within PBA/*cis*-diol polymeric complexes. These reversible, stable multiple interaction sites, in addition to a long accessible polymeric linker, enabled “reversible” control of cell adhesion by specific biomolecular exchange (e.g., glucose or fructose). This biomolecule-triggered, non-invasive strategy shows great promise for use in real-time biological research and mimics natural biomolecular feedback systems, thus having potential application in medical diagnoses and regenerative medicine.

Dynamic interactions between mammalian cells and the extracellular matrix (ECM) are exquisite characteristics of cell-level biological processes.<sup>1</sup> These interactions, which can be triggered by extracellular environmental changes or specific biomolecules, can promote specific cell signaling and biochemical cascades, consequently inducing relevant cell behaviors, such as adhesion, migration, differentiation, and apoptosis. To mimic such a molecularly dynamic and reversible ECM, sophisticated synthetic biointerfaces with dynamic display of bioactive molecules have attracted attention because of their significance in real-time cell biology research and regenerative medicine.<sup>1,2</sup>

Because cell adhesion is a prerequisite for other cell behaviors during the growth of most mammalian cells, dynamically functionalized matrices with cell-adhesive factor RGD peptide (Arg-Gly-Asp) have been extensively studied.<sup>2b,e</sup> Studies have shown that the bioactivity of some covalently bound RGD can be switched by means of temperature,<sup>3</sup> electrochemical potential,<sup>4</sup> chemical reactions,<sup>5</sup> and UV light.<sup>6</sup> In particular, reversible changes in surface molecular geometry through the conversion of electrical potential<sup>4</sup> or the photoisomerization of azobenzene<sup>6a,c</sup> can result in “reversible” control of cell adhesion by mediating the accessibility of surface covalently immobilized RGD motifs. Such kinds of reversible cell adhesion, however, are extremely rare and may be invasive, thus it is an area still in its infancy. Another promising approach to realize dynamic cell adhesion is to employ a noncovalent method, a naturally reversible interaction, to introduce adhesive factors. However, current

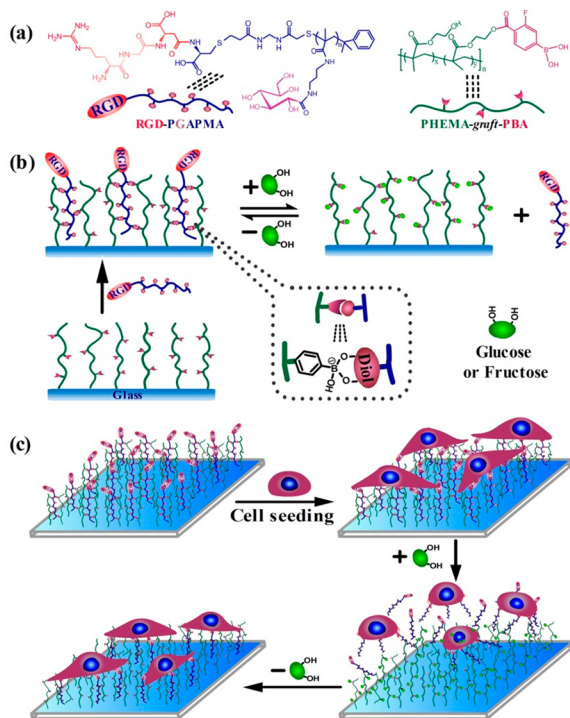
attempts, including host–guest supermolecular chemistry,<sup>7</sup> electrostatic interactions,<sup>8</sup> hydrogen bonding<sup>9</sup> and a bioimprinting technology,<sup>10</sup> merely achieve unidirectional control of cells from adhesion to release unless the biointerface is retreated. In addition to the low association constant of noncovalent bonds (leading to leakage of the factors), these processes also involve a release of surface-bound adhesive factors. Despite part of such released factors still being conjugated with the released cells (drawbacks in these systems include relatively low binding forces of noncovalent bonds and limited binding sites), the inaccessibility of such binding sites on the cell surface could make it difficult to be recruited repeatedly by the biointerfaces. Thus, it remains a significant challenge to fabricate dynamic biointerfaces or ECM mimics for reversible control of cell behaviors based on current approaches.

Reversible covalent bonds between phenylboronic acid (PBA) and 1,2-/1,3-*cis*-diols in aqueous solution are widely used for the construction of molecular receptors.<sup>11</sup> PBA/*cis*-diol polymeric complexes thus possess advantages such as reversible, stable multiple interaction sites, and long accessible polymer chains. Therefore, in this work, we present, for the first time, a method for dynamic introduction of bioactivity onto a matrix via reversible multicovalent interactions in PBA/*cis*-diol polymeric complexes. In our design, we fabricated a functionalized substrate with PBA-containing polymer brushes and designed a modified RGD peptide that conjugated with a synthetic glycopolymer chain (Scheme 1a,b). Using our method, the modified RGD was stably immobilized on the substrate by virtue of multicovalent interactions between the PBA groups in grafted polymer brushes and the *cis*-diol groups in glycopolymers. Reversible binding of the modified RGD was easily achieved by adding the medium with specific biomolecules containing *cis*-diol groups (e.g., glucose or fructose), which could exchange with glycopolymer chains,<sup>11d,e</sup> thus leading to biomolecule-triggered release of RGD and subsequent cell release (Scheme 1b,c). More importantly, the accessibility of surface-conjugated long glycopolymer chains and their stable multiple interaction sites facilitated molecular exchange and surface recruitment, allowing reversible adhesion of the released cells in our system to occur when the medium was recovered to initial physiological sugar concentration. The

Received: February 23, 2014

Published: April 17, 2014

**Scheme 1. (a) Chemical Structures of RGD-PGAPMA and PHEMA-graft-PBA; (b) Schematic Illustration of Dynamic Introduction of RGD-PGAPMA on PHEMA-graft-PBA-Modified Matrix via Reversible Multivalent PBA/*cis*-Diol Complexes; (c) Reversible Control of Cell Adhesion by Specific Biomolecules (e.g., Glucose and Fructose)**



approach presented here is not only the first demonstration of reversible control of cell adhesion through reversible multivalent interactions but also the first example of dynamic display of bioactivity regulated by specific natural small biomolecules. Therefore, this approach may enable us to mimic natural biomolecular feedback systems and develop platforms for real-time cell biology research and biomedical applications.

The fabrication of this dynamic biointerface is outlined in detail in Supporting Information (Schemes S1 and S2). In this method, an initiator immobilized glass slide was first grafted with poly(hydroxyethyl methacrylate) (PHEMA) via a surface-initiated activator generated by electron transfer atom transfer radical polymerization (AGET-ATRP) following esterification of the hydroxyl with 4-carboxy-3-fluorophenylboronic acid (CFPBA), forming a layer of PHEMA-graft-PBA polymer brushes (Scheme S1). The CFPBA can form a stable complex with *cis*-diol at physiological pH,<sup>11d</sup> and PHEMA was chosen because of its inherently cell-repellant property.<sup>12</sup> Meanwhile, reversible addition-fragmentation chain transfer polymerization (RAFT) of 3-gluconamidopropyl methacrylamide (GAPMA) was carried out. The thioester end group of the resultant poly(GAPMA) (PGAPMA) was then reduced to thiol and bridge-connected to a thiol-terminated peptide RGDC (Arg-Gly-Asp-Cys) by *N,N'*-methylene bis(acrylamide) (MBA) via thiol-ene click chemistry, finally obtaining an RGD-capped gapopolymer (RGD-PGAPMA) (Scheme S2).

The glass slides were then characterized by ellipsometry, X-ray photoelectron spectroscopy, and static contact angle experiments. Significant increases in the thickness (around 20 nm) and boron element content of surface-grafted layers confirmed the

successful grafting of PHEMA-graft-PBA brushes (Table S1, Figures S1 and S2). More importantly, we found a gradual increase in surface hydrophilicity as the PHEMA-modified glass was grafted with increasing amounts of CFPBA (Table S1). For example, the average water contact angles of a pure PHEMA-modified surface (Glass-PBA<sub>0</sub>) and a typical PBA-grafted surface (Glass-PBA<sub>400</sub>) were 47.5 and 29.1°, respectively (Figure 1a).

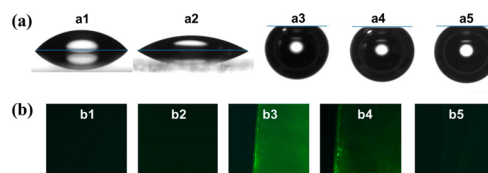


**Figure 1. (a) Water drop profiles on Glass-PBA<sub>0</sub> (a1), Glass-PBA<sub>400</sub> (a2), and air bubble profiles below Glass-PBA<sub>400</sub> in pure PBS (a3), PBS containing 60 mM glucose (a4) and 60 mM fructose (a5). For bubble tests, the measurements were carried out after immersion of the slides in different PBS (pH = 7.4) for 15 min. (b) Images of fluorescently labeled Glass-PBA<sub>0</sub> (b1), Glass-PBA<sub>400</sub> coupled with RGE-PGAPMA<sub>10</sub> (b2), Glass-PBA<sub>400</sub> with RGD-PGAPMA<sub>10</sub> before (b3) and after incubated in 60 mM glucose (b4) and fructose (b5) for 1 h.**

This peculiarity could be attributed to the polyhydroxyl groups in boric acid and will be useful to improve the cell-repellant property and reduce nonspecific cell adhesion, as shown below. Bubble contact angle experiments also showed increases in the hydrophilicity of Glass-PBA<sub>400</sub> if the slides were incubated in PBS containing specific *cis*-diol biomolecules (glucose or fructose, 60 mM in PBS, pH = 7.4) (Figure 1a). These results clearly demonstrated the saccharide responsiveness of Glass-PBA<sub>400</sub> at physiological pH due to the formation of PBA/*cis*-diol complexes.<sup>13</sup> As another part of our system, four peptide-capped PGAPMA polymers with different degrees of polymerization (RGD-PGAPMA<sub>10</sub>, RGD-PGAPMA<sub>23</sub>, RGD-PGAPMA<sub>43</sub>, and biologically inactive control RGE-PGAPMA<sub>10</sub>) and all with low polydispersity index were obtained via RAFT polymerization (Tables S2 and S3, Figures S4–S6).

Considering that GAPMA and CFPBA can form PBA/*cis*-diol complexes at physiological pH (Figure S3), we first investigated the dynamic binding of RGD-capped PGAPMA on the glass slides. Glass-PBA<sub>0</sub> and Glass-PBA<sub>400</sub> were chosen and incubated in PBS (pH = 7.4) containing 1 mM RGD-PGAPMA<sub>10</sub> or RGE-PGAPMA<sub>10</sub>. After 1 h of incubation, the glass slides were covered with a mixture of integrin  $\alpha_v\beta_3$  and AF488-labeled  $\alpha_v\beta_3$  antibody (1:1 molar ratio in PBS), then washed and examined under a fluorescence microscope. Integrin  $\alpha_v\beta_3$  can specifically recognize the RGD peptide,<sup>14</sup> thus enabling introduction of fluorescently labeled  $\alpha_v\beta_3$  antibody on an RGD peptide immobilized surface. We found that Glass-PBA<sub>400</sub> coupled with RGD-PGAPMA<sub>10</sub> exhibited strong green fluorescence, while Glass-PBA<sub>0</sub> alone or Glass-PBA<sub>400</sub> coupled with biologically inactive RGE-PGAPMA did not (Figure 1b). Previous studies also revealed that the dynamic interaction of PBA/*cis*-diol complexes could be easily achieved via molecular exchange.<sup>11d,e</sup> Therefore, fluorescently labeled Glass-PBA<sub>400</sub> was further treated with glucose or fructose. Because subsequent cell culture experiments were carried out in low-glucose Dulbecco's modified Eagle's medium (DMEM, 5.6 mM of glucose, within the physiological sugar concentration), we used PBS containing 5.6 mM glucose as a control. Our data clearly demonstrated that the observed strong fluorescent signal did not weaken for up to 12 h in the control (data not shown), while the intensity dramatically diminished in 1 h following

incubation of the glass slides with PBS containing 60 mM glucose or fructose (Figure 1b). Moreover, due to the higher association constant of PBA/fructose complexes,<sup>15</sup> the extent of weakening was more intense for fructose than for glucose. These results confirmed that bioactive RGD-PGAPMA glycopolymers could be stably immobilized on the PHEMA-*graft*-PBA functionalized substrate through the formation of PBA/*cis*-diol complexes and then released via specific biomolecule exchange, thus exhibiting dynamic display of bioactive RGD peptide on the fabricated biointerface.

The ability of cells to adhere on the functionalized glass slides was investigated by incubating with MG63 cells in low-glucose DMEM. Glass-PBA<sub>400</sub> exhibited more efficient cell repulsion than Glass-PBA<sub>0</sub> in 3 h (Figures 2a and S7), mainly due to its

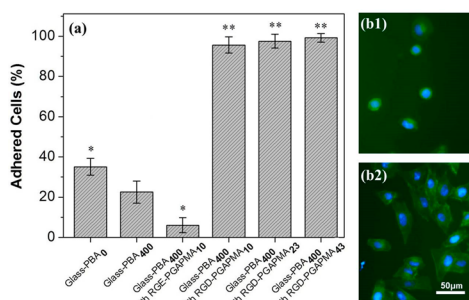


**Figure 2.** (a) Cell adhesion efficiency of MG63 on different surfaces after 3 h culturing. For peptide coupled surfaces, the slides were incubated in different peptide–PGAPMA solutions for 1 h (1 mM in PBS, pH = 7.4). Cell adhesion efficiency on tissue culture plates (TCPs) was defined as 100%. Statistical significance given compares samples to the control uncoupled Glass-PBA<sub>400</sub>; \*\* $p < 0.001$ , \* $p < 0.05$ . (b) Representative fluorescence micrographs of MG63 cells on Glass-PBA<sub>400</sub> (b1) and Glass-PBA<sub>400</sub> with RGD-PGAPMA<sub>10</sub> (b2).

increased surface hydrophilicity (Figure 1a). This also indicated that the PBA groups in our system have almost no influence on cell adhesion in spite of the existence of polysaccharides on the cell surface (Figure S13). Thus, Glass-PBA<sub>400</sub> was chosen for subsequent experiments. RGD peptides conjugated with three different lengths of PGAPMA were coupled on Glass-PBA<sub>400</sub> for cell adhesion. After 3 h of culture, they all showed significant increases in cell adhesion and spreading properties as compared to uncoupled Glass-PBA<sub>400</sub> or Glass-PBA<sub>400</sub> coupled with inactive RGE-PGAPMA<sub>10</sub> (Figures 2a and S8). We further applied DAPI and phalloidin reagents for staining of nuclei and F-actin molecules, respectively. Observation of the organization of F-actin networks for cells adhered to glass slides modified with the three RGD-PGAPMA polymers showed that the adhered cells exhibited typical focal adhesion patterns (Figures 2b and S9). These results clearly demonstrated that surface coupling of an RGD peptide through PBA/*cis*-diol complexes was a robust strategy for specific cell adhesion.

Next, cell release from Glass-PBA<sub>400</sub> was examined to determine whether this process could be triggered by glucose or fructose via a molecule-exchange process. First, we investigated Glass-PBA<sub>400</sub> coupled with RGD-PGAPMA<sub>10</sub>. After 3 h of incubation to allow cell spreading, the initial low-glucose DMEM was changed to DMEM containing 60 mM glucose or fructose. As clearly shown in Figure 3, gradual transition of the cell morphology from a spread-out shape to a round shape was clearly observed in both the glucose- and fructose-containing DMEM, demonstrating significant biomole-

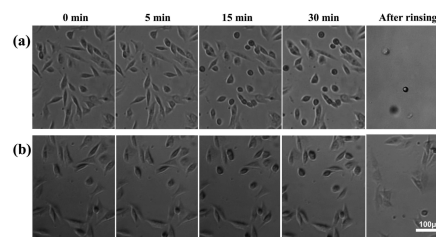


**Figure 3.** MG63 cell release from RGD-PGAPMA<sub>10</sub> coupled Glass-PBA<sub>400</sub> at different times by incubation with 60 mM fructose (a) and glucose (b).

cule-triggered cell release properties of this system. Interestingly, fructose exhibited better MG63 release efficiency compared to glucose. Specifically, about 64% of the cells were released in fructose-containing DMEM after 30 min of incubation, while only 27% of the cells were released in glucose-containing medium (Figure S10). This is mainly due to the relatively high association constant of PBA/fructose complexes and therefore rapid RGD release kinetics (Figure S12). Further, to check the applicability of our method, another cell line (annulus fibrosus stem cells from rabbit) was also used. Similarly, they both showed significant specific cell adhesion and release when sugars are added (Figures S14–S16). This result indicates that the reversible PBA/*cis*-diol complexes in our system can be used as a general approach to fabricating dynamic biointerface.

To investigate whether the released cells were able to re-adhere on the matrix, we refreshed the medium with the initial low-glucose DMEM. Notably, in the absence of sufficient sugar molecules in the medium, almost all of the released cells re-adhered on the glass in 6 h, exhibiting a clear reversible cell adhesion process (Figure 4a,b). Taken together, these findings

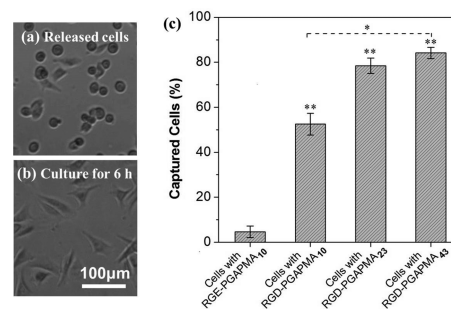


**Figure 4.** (a) Released MG63 from RGD-PGAPMA<sub>10</sub> coupled Glass-PBA<sub>400</sub> after 1 h of incubation in DMEM with 60 mM fructose. (b) Re-adhesion of the released MG63 after 6 h of culture in low-glucose DMEM. (c) Cell adhesion efficiency on Glass-PBA<sub>400</sub> after the cells were pre-conjugated with different peptide-capped glycopolymers (0.1 mM in PBS). Cells were cultured in low-glucose DMEM for 6 h. RGE-PGAPMA<sub>10</sub> was used as control; \*\* $p < 0.001$ , \* $p < 0.05$ . The number of unconjugated cells adhered on TCP was defined as 100%.

demonstrated that our system allowed for a dynamic, reversible cell adhesion behavior and that cells within our system remained viable, supporting that this biomolecule-triggered process was noninvasive.

To further explain this effect, the influence of glycopolymer chain length on cell adhesion and release behaviors was investigated. Although RGD peptides conjugated with different lengths of PGAPMA showed no obvious differences in cell adhesion (Figure 2a), the cell release efficiency was highly dependent on the chain length of the glycopolymer. Longer



glycopolymers were more beneficial to stable cell adhesion and thus harder to release (Figure S10). In line with previous results,<sup>16</sup> we also found an enhancement in cell adhesion when cells were pre-conjugated with long RGD-PGAPMA glycopolymers through RGD–integrin interactions. In this case, cells could efficiently adhere on the uncoupled Glass-PBA<sub>400</sub> despite its cell repulsion properties (Figure S11). For instance, the percentage of adhered cells increased from 52% for RGD-PGAPMA<sub>10</sub> (2.5 nm in length) to 84% for RGD-PGAPMA<sub>43</sub> (10.8 nm in length) (Figure 4c and Table S3). This significant enhancement in cell adhesion showed that cells conjugated with longer glycopolymers could be more efficiently captured by the substrate, probably due to the increased number of interaction sites and the accessibility of long glycopolymers chains. This is consistent with a recently reported “multivalent DNA network”,<sup>17</sup> in which long repeating aptamer domains exhibited higher cell capture efficiency than short monovalent aptamers. In a similar fashion, the cell re-adhesion properties of our system were expected because the released cells still readily conjugated with long glycopolymers chains. However, the second round of cell re-adhesion was not as efficient as the first round unless RGD-PGAPMA glycopolymers were re-added to the medium, probably due to the consumption of RGD peptide during the replacement of cell culture medium.

In conclusion, we have developed a dynamic biointerface immobilized with cell adhesive factor via reversible multivalent interactions of PBA/*cis*-diol polymeric complexes. Due to the presence of multiple reversible, stable interaction sites as well as long accessible polymer chains, reversible cell adhesion behavior was achieved in a noninvasive fashion by specific biomolecular exchange. In addition to the significance in real-time studies of biological processes, this specific biomolecule-triggered dynamic biointerface also acts as a mimic of natural biomolecular feedback systems. Moreover, considering the multiple strong interactions in PBA/*cis*-diol polymeric complexes, this approach provides a more promising method for both stable and dynamic immobilization of bulky biomacromolecules, such as DNA, RNA, and proteins on artificial ECMs, and therefore has great promise for use in the fields of medical diagnostics and regenerative medicine.

## ■ ASSOCIATED CONTENT

### Supporting Information

Materials and methods, supporting data. This material is available free of charge via the Internet at <http://pubs.acs.org>.

## ■ AUTHOR INFORMATION

### Corresponding Author

yueer@suda.edu.cn

### Notes

The authors declare no competing financial interest.

## ■ ACKNOWLEDGMENTS

This work is supported by the National Natural Science Foundation of China (21204056), Natural Science Foundation of Jiangsu Province (BK2012173), China Scholarship Council (201308320113), and China Postdoctoral Science Foundation funded project (2012M520060, 2013T60555).

## ■ REFERENCES

- (1) (a) Huebsch, N.; Mooney, D. J. *Nature* **2009**, *462*, 426–432. (b) Daley, W. P.; Peters, S. B.; Larsen, M. J. *Cell Sci.* **2008**, *121*, 255–264.
- (2) (a) Kim, J.; Hayward, R. C. *Trends Biotechnol.* **2012**, *30*, 426–439. (b) Robertus, J.; Browne, W. R.; Feringa, B. L. *Chem. Soc. Rev.* **2010**, *39*, 354–378. (c) Collier, J. H. *Soft Matter* **2008**, *4*, 2310–2315. (d) Mager, M. D.; LaPointe, V.; Stevens, M. M. *Nat. Chem.* **2011**, *3*, 582–589. (e) Mendes, P. M. *Chem. Soc. Rev.* **2008**, *37*, 2512–2529.
- (3) Hatakeyama, H.; Kikuchi, A.; Yamato, M.; Okano, T. *Biomaterials* **2006**, *27*, 5069–5078.
- (4) Ng, C. C. A.; Magenau, A.; Ngalim, S. H.; Ciampi, S.; Chockalingham, M.; Harper, J. B.; Gaus, K.; Gooding, J. J. *Angew. Chem., Int. Ed.* **2012**, *51*, 7706–7710.
- (5) (a) Zhao, C.; Witte, I.; Wittstock, G. *Angew. Chem., Int. Ed.* **2006**, *45*, 5469–5471. (b) Luo, W.; Yousef, M. N. *J. Am. Chem. Soc.* **2011**, *133*, 10780–10783.
- (6) (a) Auernheimer, J.; Dahmen, C.; Hersel, U.; Bausch, A.; Kessler, H. *J. Am. Chem. Soc.* **2005**, *127*, 16107–16110. (b) Wirkner, M.; Weis, S.; San Miguel, V.; Álvarez, M.; Gropeanu, R. A.; Salierno, M.; Sartoris, A.; Unger, R. E.; Kirkpatrick, C. J.; del Campo, A. *ChemBioChem* **2011**, *12*, 2623–2629. (c) Liu, D.; Xie, Y.; Shao, H.; Jiang, X. *Angew. Chem., Int. Ed.* **2009**, *48*, 4406–4408. (d) Ohmuro-Matsuyama, Y.; Tatsu, Y. *Angew. Chem., Int. Ed.* **2008**, *47*, 7527–7529.
- (7) (a) Sheng, W.; Chen, T.; Tan, W.; Fan, Z. H. *ACS Nano* **2013**, *7*, 7067–7076. (b) Boekhoven, J.; Rubert Pérez, C. M.; Sur, S.; Worthy, A.; Stupp, S. I. *Angew. Chem., Int. Ed.* **2013**, *52*, 12077–12080. (c) Sur, S.; Matson, J. B.; Webber, M. J.; Newcomb, C. J.; Stupp, S. I. *ACS Nano* **2012**, *6*, 10776–10785. (d) An, Q.; Brinkmann, J.; Huskens, J.; Krabbenborg, S.; de Boer, J.; Jonkheijm, P. *Angew. Chem., Int. Ed.* **2012**, *51*, 12233–12237. (e) Seo, J.-H.; Kakinoki, S.; Inoue, Y.; Yamaoka, T.; Ishihara, K.; Yui, N. *J. Am. Chem. Soc.* **2013**, *135*, 5513–5516. (f) Sánchez-Cortés, J.; Bähr, K.; Mrksich, M. *J. Am. Chem. Soc.* **2010**, *132*, 9733–9737.
- (8) Guillaume-Gentil, O.; Akiyama, Y.; Schuler, M.; Tang, C.; Textor, M.; Yamato, M.; Okano, T.; Vörös, J. *Adv. Mater.* **2008**, *20*, 560–565.
- (9) Li, W.; Wang, J.; Ren, J.; Qu, X. *Angew. Chem., Int. Ed.* **2013**, *52*, 6726–6730.
- (10) Pan, G.; Guo, Q.; Ma, Y.; Yang, H.; Li, B. *Angew. Chem., Int. Ed.* **2013**, *52*, 6907–6911.
- (11) (a) Deshayes, S.; Cabral, H.; Ishii, T.; Miura, Y.; Kobayashi, S.; Yamashita, T.; Matsumoto, A.; Miyahara, Y.; Nishiyama, N.; Kataoka, K. *J. Am. Chem. Soc.* **2013**, *135*, 15501–15507. (b) Zhang, C.; Losego, M. D.; Braun, P. V. *Chem. Mater.* **2013**, *25*, 3239–3250. (c) Liu, H.; Li, Y.; Sun, K.; Fan, J.; Zhang, P.; Meng, J.; Wang, S.; Jiang, L. *J. Am. Chem. Soc.* **2013**, *135*, 7603–7609. (d) Matsumoto, A.; Ishii, T.; Nishida, J.; Matsumoto, H.; Kataoka, K.; Miyahara, Y. *Angew. Chem., Int. Ed.* **2012**, *51*, 2124–2128. (e) Kim, H.; Kang, Y. J.; Kang, S.; Kim, K. T. *J. Am. Chem. Soc.* **2012**, *134*, 4030–4033.
- (12) Bhat, R. R.; Chaney, B. N.; Rowley, J.; Liebmann-Vinson, A.; Genzer, J. *Adv. Mater.* **2005**, *17*, 2802–2807.
- (13) Sun, T.; Qing, G. *Adv. Mater.* **2011**, *23*, H57–H77.
- (14) Haubner, R.; Gratias, R.; Diefenbach, B.; Goodman, S. L.; Jonczyk, A.; Kessler, H. *J. Am. Chem. Soc.* **1996**, *118*, 7461–7472.
- (15) Yan, J.; Springsteen, G.; Deeter, S.; Wang, B. *Tetrahedron* **2004**, *60*, 11205–11209.
- (16) Selden, N. S.; Todhunter, M. E.; Jee, N. Y.; Liu, J. S.; Broaders, K. E.; Gartner, Z. J. *J. Am. Chem. Soc.* **2011**, *134*, 765–768.
- (17) Zhao, W.; Cui, C. H.; Bose, S.; Guo, D.; Shen, C.; Wong, W. P.; Halvorsen, K.; Farokhzad, O. C.; Teo, G. S. L.; Phillips, J. A.; Dorfman, D. M.; Karnik, R.; Karp, J. M. *Proc. Natl. Acad. Sci. U.S.A.* **2012**, *109*, 19626–19631.